

ARTICLES

An Exploration of the Relationship between Solvation Dynamics and Spectrally Determined Solvent Response Functions by Computer Simulation**Benjamin J. Schwartz* and Peter J. Rossky****Department of Chemistry and Biochemistry, The University of Texas at Austin, Austin, Texas 78712-1167**Received: September 26, 1994; In Final Form: December 6, 1994*[⊗]

The microscopic connections between solvation dynamics and the experimentally measured dynamic emission Stokes shift are explored by molecular dynamics simulation using the hydrated electron as a fully quantum mechanical probe. Solvent response functions are computed using the method of spectral reconstruction at various time resolutions for both fluorescence and stimulated emission and compared directly to the dynamic evolution of the underlying electronic energy gap. The first spectral moment proves to be a better choice of characteristic frequency than the spectral maximum, and iterative deconvolution is found to significantly improve the spectrally determined solvent response function. Use of the appropriate characteristic frequency at zero time to produce solvent response functions which do not start at unity further improves the agreement between the spectrally determined and microscopic solvent response functions.

I. Introduction

The critical role played by the solvent in solution phase chemical reactions has prompted an explosion of recent interest in solvation dynamics.¹ On the one hand, theory has demonstrated the roles of both individual and collective solvent molecule motions in solvent relaxation on different time scales.² Formal developments have linked the response of solute electronic energy levels to specific motions along solvent coordinates.³ On the other hand, experiments have investigated solvation in a wide variety of solute/solvent systems.⁴ Ultrafast spectroscopic techniques have provided experimental access^{5,6} to the inertial solvent motions which dominate the early time dynamics of solvent relaxation.^{7,8} The present work addresses the connection between these theoretical and experimental advances, focusing on the relationship between the theoretically important microscopic quantum electronic energy gap of the solute and the ultrafast transient emission spectra measured in the laboratory.

In a typical solvation experiment, time-resolved fluorescence is used to monitor the solvent relaxation around probe molecules (usually organic dyes) following the change in electronic charge distribution which occurs upon photoexcitation.^{1,4} The idea underlying this experiment is straightforward. Initially, the solvent nuclear coordinates are at equilibrium with the electronic ground state of the probe molecule. Photoexcitation of the probe occurs instantaneously on the time scale of solvent nuclear motion, placing the solvent coordinates out of equilibrium with the probe's excited state electronic charge distribution. As the solvent responds to this electronic perturbation, the energy of the occupied excited electronic state is lowered as the solvent approaches equilibrium with the new charge distribution, while the energy of the unoccupied ground state increases as the solvent moves further away from its former ground state equilibrium configuration. The net result is that the quantum electronic energy gap of the probe continuously decreases as the solvent responds. This change in electronic energy is

reflected in the time-dependent Stokes shift of the probe fluorescence observed in the laboratory.

There are two principal drawbacks to using this seemingly straightforward experiment to explore solvation. First, the solvent response contains an ultrafast inertial component that occurs on a time scale which is comparable to or faster than the best instrumental resolution presently available.^{5–7} This results in solvation dynamics that occur on different time scales being convoluted together in the measured time-dependent spectra. Indeed, the reported solvation times for many systems have decreased in nearly direct proportion to improvements in experimental time resolution.¹ Second and more importantly, there is no simple relationship between the instantaneous emission spectra measured in the laboratory and the microscopic quantum energy gap of the probe molecule. The instantaneous fluorescence spectra of most probe molecules are broad and asymmetric, making the choice of any particular frequency (such as the emission peak or the first moment of the entire spectrum) as representative of the quantum energy gap somewhat arbitrary. Moreover, the width, shape, and intensity of the emission spectrum change as solvation proceeds, causing different choices of characteristic frequency to produce different spectrally determined solvent response functions.^{1,9}

This variability of the emission spectrum with solvation is due to a variety of microscopic factors. Non-Condon effects (variations in the emission intensity with the solvent coordinates) can skew the emission spectra toward particular energies with favorable transition dipoles independent of the position of the underlying quantum energy gap. Probe molecule polarizability¹⁰ (changes in the electronic structure of the probe resulting from the solvent response) can alter the basic shape of the probe emission spectrum and masquerade as simple solvation dynamics. The distribution of sites available to the probe molecules may also change with solvation, obscuring the quantum dynamics beneath the evolving inhomogeneity. Finally, the normal ω^3 intensity variation of spontaneous emission causes an additional change in spectral shape as the fluorescence red-shifts,¹¹ an effect which may be especially important when

[⊗] Abstract published in *Advance ACS Abstracts*, February 15, 1995.

probes with large total Stokes shifts are utilized as measures of solvation dynamics.

Clearly, what is needed is a direct comparison of the time evolution of the quantum electronic energy gap of a probe with solvent response functions computed from the time-dependent Stokes shift for different time resolutions and choices of characteristic frequency. In this paper, we use the results of quantum molecular dynamics simulations to make such a comparison. The simulations take advantage of a fully quantum mechanical probe, the hydrated electron, to compute the change in quantum electronic energy with solvation following photoexcitation. Time-dependent emission spectra are determined directly from the quantum wave functions, incorporating the full range of non-Condon, inhomogeneous site distribution and solute polarizability effects.¹² These emission spectra are calculated for several simulated instrument resolutions, and we examine the adequacy of using these directly computed spectra to represent the dynamics of the underlying quantum energy gap. To further study the effects of limited time resolution, we also use an iterative convolute-and-compare fitting method to deconvolute the calculated emission transients in the time domain before performing spectral reconstruction⁹ in a manner identical to the treatment of experimental data. We find that the first moment of the emission spectrum proves to be a better choice of characteristic frequency than the emission maximum and that the ω^3 factor for spontaneous emission plays relatively little role in the computed solvent response function. We also find that deconvolution in the spectral reconstruction procedure provides a significant enhancement in capturing the early portions of the solvent response and that proper choice of the zero time characteristic frequency can lead to a marked improvement in the spectrally determined solvent response function.

II. Methods

The simulation techniques we employ are identical to those used in our previous studies,¹³ so we describe them only briefly here. The system was modeled by 200 classical simple point charge water molecules with the addition of internal flexibility¹⁴ and one quantum electron in a cubic cell of side 18.17 Å (density 0.997 g/mL) with standard periodic boundary conditions at a temperature of 300 K. The electron-water interactions were described by a pseudopotential,¹⁵ and quantum dynamics were performed using the nonadiabatic algorithm of Webster *et al.*¹⁶ The equations of motions were integrated using the Verlet algorithm¹⁷ with a 1 fs time step. Spectral calculations included the 40 lowest adiabatic eigenstates, computed on a 16^3 grid with an efficient iterative and block Lanczos scheme.¹⁶ The transition dipoles computed in this manner indicate that non-Condon effects are of importance in the spectroscopy of the hydrated electron.¹⁸

The simulations model equilibrium ground state hydrated electrons photoexcited by an ultrafast laser pulse centered at 2.27 eV, in close parallel with the recent experimental investigations of Barbara and co-workers.¹⁹ The change in the quantum energy gap, $U(t)$, following photoexcitation and the dependence of this change on the molecular details of the solvent response have been discussed in detail in a previous report.¹³ For the hydrated electron, the nonequilibrium solvent response function given by

$$S(t) = \frac{U(t) - U(\infty)}{U(0) - U(\infty)} \quad (1)$$

is well characterized by a 24 fs Gaussian inertial component (38%) superimposed on a 240 fs exponential decay (62%). The calculated time-dependent stimulated emission spectra following excitation have also been presented previously¹³ and provide the starting point for the present comparison between the time evolution of the quantum energy gap and the dynamic spectral Stokes shift. To avoid confusion, we introduce two additional spectral solvent response functions based on the choice of either the emission maximum or the first spectral moment as the characteristic frequency:

$$S_{\text{pk}}(t) = \frac{\omega_{\text{pk}}(t) - \omega_{\text{pk}}(\infty)}{\omega_{\text{pk}}(0) - \omega_{\text{pk}}(\infty)} \quad (2)$$

$$S_{\text{av}}(t) = \frac{\bar{\omega}(t) - \bar{\omega}(\infty)}{\bar{\omega}(0) - \bar{\omega}(\infty)} \quad (3)$$

where $\omega_{\text{pk}}(t)$ is the peak frequency of the emission at time t and $\bar{\omega}$ is the average emission frequency at time t .

Due to the nature of the fluorescence up-conversion technique, most experimental time-resolved emission data are taken one wavelength at a time. This requires weighting the transients measured at different frequencies appropriately to accurately determine the instantaneous emission spectrum at a given time. Typically, the method of spectral reconstruction is used,⁹ in which the time domain transients are fit to multiple exponentials convoluted with the instrument response, and the time integral of the fit at each frequency is weighted by the corresponding intensity of the static fluorescence spectrum. The weighted instantaneous spectra are computed from the deconvoluted time domain fitting parameters and then fit in the frequency domain to a continuous function, usually a log-normal distribution.²⁰ This provides an analytic representation of the data which is useful for interpolating between measured wavelengths to determine the position of the spectral maximum or average. The solvent response function is then determined via eq 2 or 3 from the fits to the reconstructed frequency domain spectra.

In analyzing our simulated emission transients, we have made some slight modifications to the standard spectral reconstruction procedure. Because the time domain emission traces for the hydrated electron are computed directly with absolute intensities¹³ and the static fluorescence spectrum is unknown, we have elected to bypass the portion of the experimental reconstruction process involving the spectral weighting. To investigate the role of deconvolution in the spectral reconstruction procedure, we have computed spectrally determined solvent responses both from the directly calculated instantaneous emission spectra and from emission spectra which were reconstructed from deconvoluted fits to the time domain emission transients.

III. Results and Discussion

A. Directly Calculated Instantaneous Spectra. Figure 1 displays representative nonlinear least-squares fits of the four-parameter modified log-normal distribution function²¹

$$I(\omega) = I_0 \exp\left\{-\frac{1}{2c^2}\left[\ln\left(\frac{\omega - a}{b}\right)\right]^2\right\} \quad (4)$$

to the directly calculated instantaneous stimulated emission spectra of the hydrated electron at two time delays, computed with a 100 fs Gaussian instrument response. The fits do an excellent job of representing the data, with the exception of describing the small blue spectral shoulder at early time delays. As discussed previously,¹³ this shoulder is a remnant of the immediate emission at the excitation wavelength, 2.3 eV,

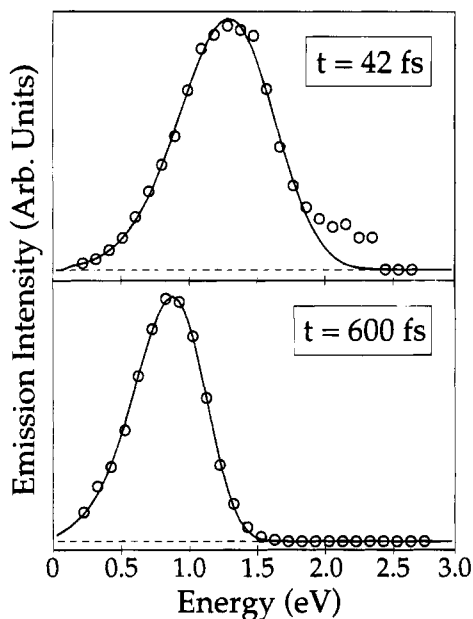


Figure 1. Instantaneous stimulated emission spectra for the hydrated electron (circles) at two time delays calculated at 100 fs time resolution. Solid curves are nonlinear least-squares fits of eq 4 to the spectral data red of 2.0 eV. The emission spectrum undergoes a strong red shift and increase in asymmetry and overall narrowing between the two times displayed.

convoluted by the instrumental resolution with the enormous Stokes shift produced by the inertial solvent response. To avoid having this shoulder (which is prominent only for times ≤ 50 fs, much less than the instrument function) interfere with the calculated spectral solvent response, only spectral data at energies < 2.0 eV were used in these log-normal fits. Comparison of the two spectra in Figure 1 also demonstrates the large Stokes shift, decrease in spectral width, and increase in asymmetry of the emission spectrum with time.

Once the instantaneous spectra at each time delay are fit to eq 4, the fit parameters can be used to determine the spectral response functions $S_{pk}(t)$ and $S_{av}(t)$. The emission maximum at each time is determined directly from the nonlinear least squares fit parameters as $\omega_{pk} = a + b$, while the first spectral moment can be determined analytically from

$$\bar{\omega} \equiv \frac{\int_{-\infty}^{\infty} \omega I(\omega) d\omega}{\int_{-\infty}^{\infty} I(\omega) d\omega} = a + b \exp\left(\frac{3}{2}c^2\right) \quad (5)$$

Figure 2 presents the spectral response functions computed via eqs 2 and 3 for the raw stimulated emission spectra calculated with both 300 fs (upper panel) and 100 fs (lower panel) Gaussian instrument functions. The solvent response function $S(t)$, determined by eq 1 using the actual quantum energy gap, is also shown for comparison. As expected, none of the spectrally determined response functions come close to reproducing the early time dynamics of the true solvation response due to insufficient time resolution, although $S_{av}(t)$ computed at 100 fs resolution does a reasonable job of capturing the longer time solvent relaxation.

Inspection of Figure 2 reveals that, at both time resolutions, $S_{av}(t)$ provides a better estimate of the quantum energy gap dynamics than does $S_{pk}(t)$. This result can be rationalized in terms of the large changes in spectral shape which take place at early times due to the convolution of the inertial and later portions of the solvent response by the instrument function. The true time zero emission spectrum for the hydrated electron is

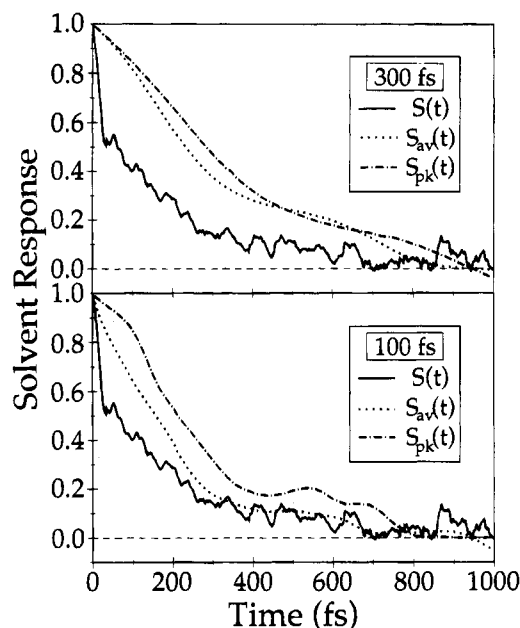


Figure 2. Comparison of the spectrally determined and microscopic solvent response functions for different time resolutions and choices of characteristic frequency. Solid curves in both panels are the quantum energy gap solvent response function, $S(t)$ (eq 1). Dotted curves show the spectrally determined solvent response when the first spectral moment is used as the characteristic frequency, $S_{av}(t)$ (eq 3). Dot-dashed curves show the spectrally determined solvent response function employing the spectral maximum as the characteristic frequency, $S_{pk}(t)$ (eq 2). Instantaneous stimulated emission spectra at 300 and 100 fs time resolution were used to obtain fitting parameters for the spectral response functions in the upper and lower panels, respectively.

simply the spectrum of the excitation pulse (essentially a delta function), since unlike molecular probes, the electron undergoes no internal relaxation after excitation. The measured early time spectra, however, are broad and diffuse, as the convolution mixes emission from a large range of electronic energy gaps. As time progresses, the convolution samples a narrower distribution of quantum transition energies, and the emission spectrum becomes narrower in time.¹³ The net result is that the nascent emission spectrum, which is peaked toward lower frequencies, becomes broader and more symmetric as time initially progresses but then narrows again and becomes asymmetric with a maximum to the blue side at later times. Thus, the peak frequency does not change nearly as much as the average frequency during this complex spectral evolution, leading to the result that $S_{pk}(t)$ does not capture the early time solvation dynamics as well as $S_{av}(t)$. This effect becomes especially pronounced when the instrumental resolution becomes comparable to the time scale of the inertial response, as seen in Figure 2.

Figure 2 also reveals the surprising fact that insufficient time resolution could actually lead to an overestimate of the importance of the inertial component of the solvent response if pursued naively. The use of characteristic spectral frequencies and the instrumental convolution results in a spectral response function with a different analytic shape than the underlying quantum solvation response. If one attempted to fit these convoluted spectral responses to Gaussian + exponential decay dynamics, it would evidently produce an overestimate of both the fractional response due to the Gaussian component and the time constants of both the exponential and Gaussian decays. This most likely results from the fact that a large portion of the inertial component of the response is missed with inadequate time resolution, so that Gaussian fits to the early time solvent response are not representative of the underlying inertial

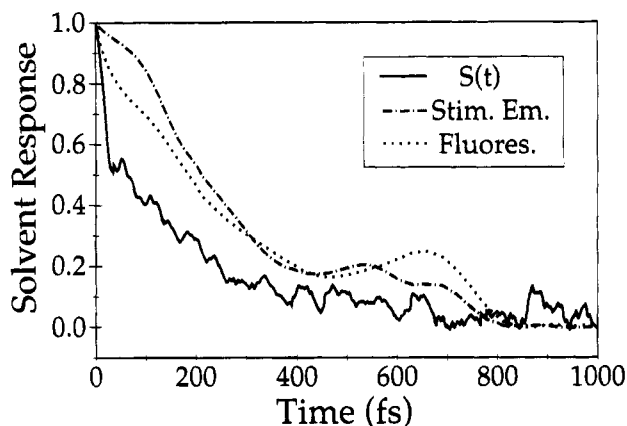


Figure 3. Comparison of the spontaneous fluorescence (dotted curve) and stimulated emission (dot-dashed curve) spectrally determined response functions using the emission maximum as the characteristic frequency, $S_{pk}(t)$ (eq 2). Instantaneous emission spectra at 100 fs time resolution were used to obtain the fitting parameters for both curves. The underlying microscopic solvent response function, $S(t)$ (eq 1), is also shown for comparison (solid curve).

solvation dynamics. For example, the spectral response function $S_{pk}(t)$ computed at 100 fs resolution fits to a 155 fs Gaussian (61%) plus a 410 fs exponential (39%), while that computed at 300 fs resolution fits somewhat more poorly to a 230 fs Gaussian (41%) plus a 435 fs exponential (59%). Both fits overestimate the actual 38% amplitude of the inertial component, with the estimate actually becoming worse at the higher time resolution which mixes the underlying inertial and exponential solvent dynamics to a greater degree. For an instrument function which is long compared to the inertial time scale, we anticipate that an initial Gaussian component would no longer fit at all to the spectrally determined solvent response, in accord with expectations of completely missing the inertial solvation dynamics.

The spectrally determined solvent response functions presented in Figure 2 were computed from stimulated emission spectra and thus do not include the ω^3 intensity variation present in experiments which measure up-converted spontaneous fluorescence. Since the relaxation of the underlying quantum energy gap bears no relation to this intensity variation, the ω^3 weighting of the spontaneous emission provides another potential discrepancy between the spectrally determined and microscopic solvent response functions.¹¹ To offer a more realistic comparison between theory and experiment, we have weighted the calculated 100 fs stimulated emission spectral data by ω^3 , refit the weighted spectra to eq 4, and used the new fitting parameters to compute fluorescence spectrally determined response functions via eqs 2 and 3. Figure 3 presents a comparison between the spectral maximum solvent response functions determined at 100 fs time resolution for both the stimulated emission ($S_{pk}^{se}(t)$) and the fluorescence spectra ($S_{pk}^{fl}(t)$). The figure shows that $S_{pk}^{fl}(t)$ initially decays a little more quickly than $S_{pk}^{se}(t)$, leading to seemingly better agreement with the underlying $S(t)$. Part of this fortuitous agreement can be explained by the fact that the ω^3 weighting blue-shifts the peak of the time-zero emission spectrum to a greater degree than the time-infinity spectrum, and thus use of fluorescence appears to capture a greater fraction of the total spectroscopic response. Most of the slightly faster initial decay of $S_{pk}^{fl}(t)$, however, is a simple reflection of the fact that the spontaneous fluorescence transition rate is higher in the blue than in the red, leading to a faster red shift of the emission maximum at early times even though this enhanced red shift is not related to the underlying solvation dynamics. Correspondingly, the somewhat lower spontaneous emission rate in the red leads to slightly poorer agreement between $S_{pk}^{fl}(t)$

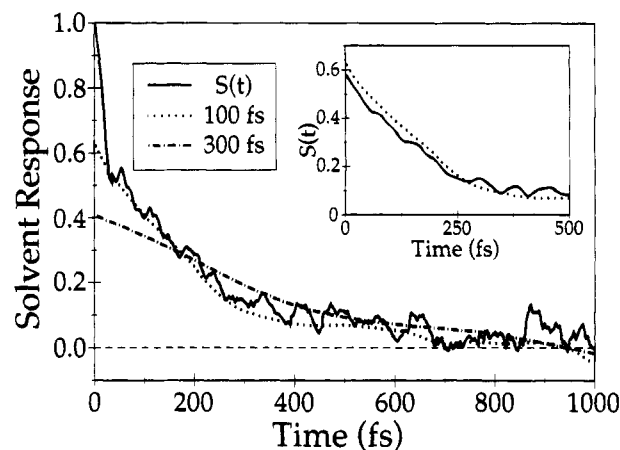


Figure 4. Comparison between the microscopic and time-zero frequency corrected spectrally determined solvent response functions. The solid curve shows the quantum energy gap determined solvent response, $S(t)$ (eq 1). The solvent response function utilizing the first spectral moment as the characteristic frequency, $S_{av}(t)$ with the $\bar{\omega}(0)$ term in the denominator of eq 3 corrected as described in the text, is calculated from fitting parameters to the instantaneous stimulated emission spectra at both 100 fs (dotted curve) and 300 fs (dot-dashed curve) time resolution. Inset: comparison of the microscopic solvent response function convoluted with the 100 fs instrument response (solid curve)²³ and the time-zero-corrected $S_{av}(t)$ calculated from the 100 fs instantaneous stimulated emission spectrum (dotted curve, same as in main figure).

and $S(t)$ at longer times. Other than this, there is qualitatively little difference between the response functions computed from the stimulated emission and fluorescence spectra, a somewhat surprising result given the enormous Stokes shift of the hydrated electron (1.71 eV, or nearly 75% of the excitation energy)¹³ and that the ω^3 factor weighting the fluorescence is not present in the dynamics of the underlying quantum energy gap.

Much of the reason for the overall poor agreement evident between the spectrally determined response functions and $S(t)$ in Figures 2 and 3 lies in the difficulty of using the instrument-convoluted emission spectra to obtain the appropriate characteristic frequency at time zero.²² Although the time zero energy gap for the electron is identical to the excitation energy, the "experimentally" measured time-zero emission spectrum is already significantly Stokes-shifted due to convolution over the inertial solvent response. This leads to spectrally determined time-zero characteristic frequencies that are quite red-shifted from the actual 2.27 eV value of the underlying time zero quantum energy gap. For the present example, $\bar{\omega}(0)$ calculated from the emission spectrum at 300 fs resolution is 1.43 eV, while $\bar{\omega}(0)$ determined at 100 fs resolution is 1.74 eV, showing that use of $\bar{\omega}$ as the characteristic frequency misses roughly 59% or 37% of the total solvent response, respectively. This problem has been recognized in the literature, and based on a comparison of static emission spectra between polar and nonpolar solvents, a prescription has been provided for estimating the proper time-zero characteristic frequency for molecular probes.²²

Figure 4 explores using this appropriate time zero characteristic frequency to improve the spectrally determined solvent response functions. The figure shows $S_{av}(t)$ computed from the stimulated emission spectra at 100 and 300 fs time resolution; only here the corrected value for $\bar{\omega}(0)$ (2.27 eV, the excitation energy) was substituted in the denominator of eq 3, while the values of $\bar{\omega}(t)$ in the numerator were calculated from the spectral fit parameters via eq 5 as before. This results in response functions which are no longer normalized to unity at zero time, but instead have initial values which directly reflect the fraction

of solvent response actually captured spectroscopically. The improvement in both spectrally determined response functions is dramatic (cf. Figure 2). The 300 fs $S_{av}(t)$ does a much better job of reproducing the long-time solvation dynamics, while the 100 fs $S_{av}(t)$ is virtually identical to the response of the quantum gap, excepting the inertial dynamics. The inset of Figure 4 compares $S(t)$ convoluted with the 100 fs Gaussian instrument function²³ to the 100 fs spectrally determined and zero-frequency corrected $S_{av}(t)$. The two functions are in complete agreement within the noise, indicating that the time-zero-corrected $S_{av}(t)$ has captured all the essential solvation information from the quantum energy gap which is available at 100 fs time resolution.

B. Deconvoluted Instantaneous Spectra. As is evident from Figures 2–4, inadequate time resolution leads to a poor representation of the early-time portions of the solvent response. This is a result of the fact that the amplitude of the rapidly decaying blue emission is underweighted due to convolution by the instrument response, leading to early-time spectra which are significantly red-shifted from the underlying value of the quantum energy gap. With knowledge of the instrument function, however, the time domain emission transients can be deconvoluted to improve the effective time resolution of the experiment. The deconvoluted fits to the early-time spectral data have much larger amplitudes in the blue than those measured directly, providing reconstructed spectra which do not miss as large a fraction of the total solvation response. Especially for rapidly responding solvents like water or methanol, determination of the solvent response from spectral data relies on both high time resolution and the ability to accurately account for the instrumental resolution by deconvolution.^{6,24}

To explore the role of deconvolution in spectral determination of the solvent response, we have computed response functions from spectra reconstructed from deconvoluted fits to the time domain emission traces. To mimic one type of possible uncertainty in the instrument response function, we computed additional time domain spectral transients convoluted with an instrument function consisting of a 100 fs Gaussian plus 5% rms amplitude noise. These time domain traces were then fit using an iterative convolute-and-compare procedure²⁵ which convoluted a (noiseless) 100 fs Gaussian assumed instrument response with either a triexponential or, in some cases, a single-exponential plus two exponentially damped sine waves.²⁶ We used the same instrument function for every wavelength and did not use the zero of time as an adjustable parameter since the absolute time zero is calculated directly from the molecular dynamics simulations. The fitting amplitudes were determined strictly by the data, and deconvoluted instantaneous spectra were reconstructed directly from the time domain fit parameters. Log-normal fits (eq 4) to the full deconvoluted spectra (energies ≤ 2.3 eV) were performed as above, with a fit quality about the same as that displayed in Figure 1.

Using the log-normal fit parameters in eqs 2 and 3, solvent response functions constructed from the deconvoluted spectral data are shown in Figure 5. The improvement in comparison to the underlying $S(t)$ from the quantum energy gap is dramatic. The deconvoluted $S_{pk}(t)$ captures most of the inertial portion of the solvent response and is also in good agreement with the noninertial part of the microscopic solvent response at later times. Nearly all of this improvement comes from amplitude enhancement of the blue wavelengths at early times in the deconvolution fitting process. The spectrally determined time-zero peak frequency is 2.11 eV, showing that the deconvolution procedure allows capture of 89% of the total solvent response, whereas only 63% of the total response was measured without deconvolution at the same time resolution. Results for the

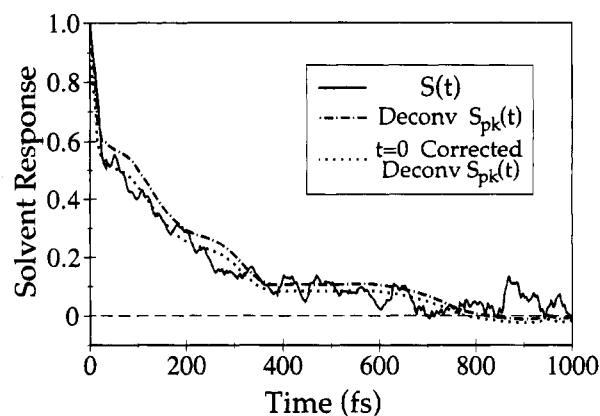


Figure 5. Comparison between the microscopic and spectrally determined solvent response functions where iterative deconvolution was used in the spectral reconstruction. The solid curve shows the underlying response of the quantum energy gap (eq 1). The deconvoluted solvent response function using the emission maximum as the characteristic frequency, $S_{pk}(t)$ (eq 2), is shown as the dot-dashed curve. The dotted curve shows the time-zero-corrected $S_{pk}(t)$, where the $\omega_{pk}(0)$ term in the denominator of eq 2 was modified as discussed in the text.

deconvoluted $S_{av}(t)$ are similar; only here the spectrally determined time-zero average frequency is 2.14 eV, representing 91% of the overall spectral shift. We note that the present exploration is of a somewhat limited nature, as for this example we are convoluting and deconvoluting the spectral data with identical instrument functions within the 5% added amplitude noise. It would be interesting, for example, to compare the effects of convoluting and deconvoluting with instrument functions that differ in their long-time tails (such as a Gaussian and Lorentzian or Gaussian and hyperbolic secant squared) on the resulting deconvoluted spectral responses.

Finally, the deconvoluted spectrally determined solvent responses can be further improved by use of the correct time zero characteristic frequency. Like the response functions presented in Figure 4, the dotted line in Figure 5 shows the deconvoluted $S_{pk}(t)$ computed using $\omega_{pk}(0) = 2.27$ eV, the excitation frequency, in the denominator of eq 2. This time zero corrected $S_{pk}(t)$ shows the changeover from inertial to noninertial behavior at the correct fraction of the solvent response. The agreement between the spectrally determined and underlying solvent responses following the inertial dynamics is also enhanced by use of the correct zero characteristic frequency.

IV. Conclusions

In summary, we have used quantum molecular dynamics simulation to compare “experimental” solvent response functions computed from the time-resolved emission spectrum to the underlying time evolution of the quantum energy gap for a realistic solvation probe, the hydrated electron. The degree of agreement between the spectrally determined and true solvent response functions, especially at early times, is a strong function of the time resolution used in measuring the emission spectra. At all time resolutions, the first spectral moment appears to be a better choice of characteristic frequency than the emission maximum for both spontaneous and stimulated emission spectra. There seems to be little difference between the stimulated emission and fluorescence spectral responses, although the slightly more rapid initial decay and greater time zero blue shift of the fluorescence mimic the capture of a slightly higher fraction of the overall solvent relaxation. With adequate knowledge of the instrument response and sufficient time

resolution, deconvolution can be used to dramatically improve the spectrally computed solvent response function. Finally, whether or not a deconvolution procedure is employed, use of the appropriate time zero characteristic frequency to produce spectral response functions which do not start at 1 leads to a notable improvement in the comparison to the desired underlying quantum solvation dynamics.

Acknowledgment. This work was supported by the National Science Foundation. We thank Graham Fleming for a critical reading of the manuscript and for making us aware of the importance of deconvolution in improving the spectral reconstruction process. B.J.S. acknowledges helpful conversations about the mechanics of deconvoluting spectral data with Ralph Jimenez and many stimulating discussions about non-Condon effects in the spectroscopy of the hydrated electron with Wayne Bosma. We thank Ralph Jimenez for providing the convolute-and-compare fitting code used in the construction of Figure 5. B.J.S. is the recipient of an NSF Postdoctoral Fellowship in Chemistry and acknowledges the allocation of computational resources from the San Diego Supercomputing Center.

References and Notes

- (1) For recent reviews, see: (a) Maroncelli, M. *J. Mol. Liq.* **1993**, *57*, 1. (b) Rossky, P. J.; Simon, J. D. *Nature* **1994**, *370*, 263. (c) Jarzaba, W.; Barbara, P. F. *Adv. Photochem.* **1990**, *15*, 1.
- (2) In addition to work cited in ref 1, see also: Stratt, R. M.; Cho, M. *H. J. Chem. Phys.* **1994**, *100*, 6700.
- (3) See, e.g.: (a) van der Zwan, G.; Hynes, J. T. *J. Phys. Chem.* **1985**, *89*, 4181. (b) Loring, R. F.; Yan, Y.; Mukamel, S. *J. Chem. Phys.* **1987**, *87*, 5840. (c) Chandra, A.; Bagchi, B. *Chem. Phys. Lett.* **1990**, *165*, 93.
- (4) See, e.g.: (a) Jarzaba, W.; Walker, G. C.; Johnson, A. E.; Barbara, P. F. *Chem. Phys.* **1991**, *152*, 57. (b) Simon, J. D. *Acc. Chem. Res.* **1988**, *21*, 128 in addition to papers cited in ref 1.
- (5) Rosenthal, S. J.; Xie, X.; Du, M.; Fleming, G. R. *J. Chem. Phys.* **1991**, *95*, 4715 as well as ref 24.
- (6) Jimenez, R.; Fleming, G. R.; Kumar, P. V.; Maroncelli, M. *Nature* **1994**, *369*, 471.
- (7) For a summary of inertial solvent dynamics, see: Maroncelli, M.; Kumar, P. V.; Papazyan, A.; Hornig, M. L.; Rosenthal, S. J.; Fleming, G. R. In *Ultrafast Reaction Dynamics and Solvent Effects*; Gauduel, Y.; Rossky, P. J., Eds.; *AIP Conf. Proc.* **1994**, *298*, 310.
- (8) A derivation that an initial Gaussian relaxation component should result from inertial solvent motions is provided in: Carter, E. A.; Hynes, J. T. *J. Chem. Phys.* **1991**, *94*, 5961.
- (9) (a) Maroncelli, M.; Fleming, G. R. *J. Chem. Phys.* **1987**, *86*, 6221. (b) Maroncelli, M.; Fleming, G. R. *J. Chem. Phys.* **1990**, *92*, 3251.
- (10) For a theoretical perspective, see: Hynes, J. T.; Kim, H. J.; Mathis, J. R.; Timoneda, J. J. *J. Mol. Liq.* **1993**, *57*, 53 and references therein.
- (11) Recent work has found that one form of inhomogeneous decay kinetics which can dominate at low temperatures is intimately related to the ω^3 intensity variation of fluorescence: (a) Fee, R. S.; Milsom, J. A.; Maroncelli, M. *J. Phys. Chem.* **1991**, *95*, 5170. (b) Maroncelli, M.; Fee, R. S.; Chapman, C. F.; Fleming, G. R. *J. Phys. Chem.* **1991**, *95*, 1012.
- (12) While we are not the first to construct time resolved emission spectra from either classical (for example, ref 8) or quantum (for example: (a) Levy, R. M.; Kitchen, D. B.; Blair, J. T.; Krogh-Jespersen, K. *J. Phys. Chem.* **1990**, *94*, 4470. (b) Muiño, P. L.; Callis, P. R. *J. Chem. Phys.* **1994**, *100*, 4093) simulations, to the best of our knowledge, previous contributions have constructed emission spectra directly from the distribution of vertical energy gaps, making explicit use of the Condon approximation. This approximation is avoided here as the emission spectral intensity, $|\langle \psi_{\text{gnd}} | \mu | \psi_{\text{ex}} \rangle|^2$, is determined directly from the quantum eigenstates as described in ref 13.
- (13) (a) Schwartz, B. J.; Rossky, P. J. *J. Chem. Phys.* **1994**, *101*, 6902. (b) Schwartz, B. J.; Rossky, P. J. *J. Chem. Phys.* **1994**, *101*, 6917.
- (14) Toukan, K.; Rahman, A. *Phys. Rev. B* **1985**, *31*, 2643.
- (15) Schnitker, J.; Rossky, P. J. *J. Chem. Phys.* **1987**, *86*, 3462.
- (16) (a) Webster, F. A.; Rossky, P. J.; Friesner, R. A. *Comput. Phys. Commun.* **1991**, *63*, 494. (b) Webster, F. A.; Wang, E. T.; Rossky, P. J.; Friesner, R. A. *J. Chem. Phys.* **1994**, *100*, 4835.
- (17) Allen, M. P.; Tildesley, D. J. *Computer Simulation of Liquids*; Oxford University Press: New York, 1987.
- (18) For the equilibrium absorption spectrum of the hydrated electron, the oscillator strength between the ground and first excited states changes noticeably due to solvent fluctuations. (The correlation between the transition dipole and frequency is roughly linear with negative slope: the oscillator strength decreases by $\sim 20\%$ over the roughly 0.5 eV range of energies sampled by solvent fluctuations.) For the stimulated emission spectra, the oscillator strength between the excited and ground states decreases by a factor of ~ 2 as the gap decreases from its initial to excited state equilibrium value with solvation.
- (19) (a) Alfano, J. C.; Walhout, P. K.; Kimura, Y.; Barbara, P. F. *J. Chem. Phys.* **1993**, *98*, 5996. (b) Kimura, Y.; Alfano, J. C.; Walhout, P. K.; Barbara, P. F. *J. Phys. Chem.* **1994**, *98*, 3450.
- (20) The log-normal distribution fits the absorption and emission bands of complex molecules surprisingly well. See, e.g.: Siano, D. B.; Metzler, D. E. *J. Chem. Phys.* **1969**, *51*, 1856.
- (21) Note that we have implicitly defined $I(\omega) \equiv 0$ whenever $\omega \leq a$, thus avoiding the natural log of zero or negative numbers. For a more complete description of the log-normal distribution and its properties, see: (a) Crow, E. L.; Shimizu, K. *Lognormal Distributions*; Marcel Dekker: New York, 1988. (b) Aitchison, J.; Brown, J. A. C. *The Lognormal Distribution*; Cambridge University Press: Cambridge, 1957).
- (22) Fee, R. S.; Maroncelli, M. *Chem. Phys.* **1994**, *183*, 235.
- (23) Note that in performing this convolution, we have assumed that $S(t)$ is given by eq 1 for $t \geq 0$, and that $S(t) \equiv 1$ for $t < 0$.
- (24) The analysis of most experimental data includes this type of deconvolution procedure. Details of the procedure as well as a discussion of the choice of the emission maximum or first spectral moment as the characteristic frequency have also been described in Rosenthal, S. J.; Jimenez, R.; Fleming, G. R.; Kumar, P. V.; Maroncelli, M. *J. Mol. Liq.* **1994**, *60*, 25 as well as in ref 9. Note that ref 6 uses a less conventional fitting procedure which globally fits the spectra to an assumed underlying functional form for $S(t)$ in the experimental derivation of a response function for water.
- (25) The convolute-and-compare fitting program, upcvfit.f, was graciously provided by Ralph Jimenez and modified to allow fitting of exponentially damped sine functions as well as simple exponential decays.
- (26) As discussed in ref 13b, the calculated time domain emission data at some wavelengths show oscillations which are the result of insufficient sampling over the phase of intermolecular solvent motions which are impulsively displaced upon photoexcitation. Exponentially damped sine waves were employed to adequately fit these traces for the iterative deconvolution procedure.

JP942599T